EFDA–JET–CP(14)01/38

A. Järvinen, , M. Groth, M. Airila, P. Belo, M. Beurskens, S. Brezinsek, M. Clever, G. Corrigan, S. Devaux, P. Drewelow, T. Eich, C. Giroud, D. Harting, A. Huber, S. Jachmich, K. Lawson, B. Lipschultz, G. Maddison, C. Maggi, T. Makkonen, C. Marchetto, S. Marsen, G.F. Matthews, A.G. Meigs, D. Moulton, M.F. Stamp, S. Wiesen, M. Wischmeier and JET EFDA contributors

Interpretation of Radiative Divertor Studies with Impurity Seeding in Type-I ELMy H-Mode Plasmas in JET-ILW Using EDGE2D-EIRENE

Interpretation of Radiative Divertor Studies with Impurity Seeding in Type-I ELMy H-Mode Plasmas in JET-ILW Using EDGE2D-EIRENE

A. Järvinen[1], , M. Groth[1], M. Airila[2], P. Belo[3], M. Beurskens[4], S. Brezinsek[5], M. Clever[5], G. Corrigan[4], S. Devaux[6], P. Drewelow[7], T. Eich[6], C. Giroud[4], D. Harting[4], A. Huber[5], S. Jachmich[8], K. Lawson[4], B. Lipschultz[9], G. Maddison[4], C. Maggi[6], T. Makkonen[1], C. Marchetto[10], S. Marsen[7], G.F. Matthews[4], A.G. Meigs[4], D. Moulton[1], M.F. Stamp[4], S. Wiesen[5], M. Wischmeier[6] and JET EFDA contributors*

JET-EFDA, Culham Science Centre, OX14 3DB, Abingdon, UK

[1]Aalto University, Association EURATOM-Tekes, Espoo, Finland
[2]Association EURATOM-Tekes, VTT Technical Research Centre of Finland, Espoo, Finland
[3]Institute of Plasmas and Nuclear Fusion, Association EURATOM-IST, Lisbon, Portugal
[4]Culham Centre of Fusion Energy, EURATOM Association, Abingdon, UK
[5]Forschungzentrum Jülich, Institut für Energie- und Klimaforschung Plasmaphysik, 52425 Jülich, Germany
[6]Max-Planck Institute for Plasma Physics, EURATOM Association, Greifswals, Germany
[7]Max-Planck Institute for Plasma Physics, EURATOM Association, Garching, Germany
[8]Association EURATOM Belgium State, Laboratory for Plasma Physics, Brussels, Belgium
[9]York Plasma Institute, University of York, Heslington, York YO10 5DD, UK
** See annex of F. Romanelli et al, "Overview of JET Results", (24th IAEA Fusion Energy Conference, San Diego, USA (2012)).*

Preprint of Paper to be submitted for publication in Proceedings of the
21st International Conference on Plasma Surface Interactions, Kanazawa, Japan
26th May 2014 – 30th May 2014

ABSTRACT

Nitrogen seeded JET-ILW H-mode plasmas have been investigated with EDGE2D-EIRENE. The simulations reproduce the experimentally observed factor of 10 reduction in the outer target power deposition when the normalized divertor radiation, P_{rad} div /P_{SOL}, increases from the unseeded levels of 15% up to the 50% levels required for detachment. At these radiation levels, nitrogen is predicted dominate the total radiation with a contribution of 85%, consistent with previous measurements in JET-C. Due to low radiative potential of nitrogen in the electron temperatures above 100eV, more than 80% of the radiation is predicted to occur in the scrape-off layer, making nitrogen a suitable divertor radiator for typical JET divertor conditions with T_e around 30 eV. The simulations reproduce the experimentally observed particle flux reduction at the low-field side target without the need for strong recombination. This is due to low power levels entering the deuterium ionization front, inaccessible without strong impurity radiation.

1. INTRODUCTION

Divertor heat load and detachment control is mandatory in the next step devices, such as ITER, to maintain surface heat fluxes below 5 – 10MW/m^2 and to minimize tungsten sputtering while operating at or above H_{98} of unity [1, 2]. Increasing divertor radiation by injecting low-Z impurities, such as nitrogen or neon, to reduce scrape-off layer heat flux and to cool the divertor plasma to detachment is put forward as the primary method to achieve this goal. Such radiative dissipation must be achieved with acceptable consequences for the plasma performance in terms of confinement, radiative cooling and dilution of the burning plasmas. While there is qualitative understanding of the physics processes occurring in impurity seeding to detachment, most of this understanding is based on analytic, one-dimensional models. Furthermore, quantitative understanding of the magnitude, hierarchy, and interplay of the various processes is challenging to obtain experimentally. Therefore, quantification of these processes with 2D validated numerical models is required to further enhance the understanding of detached radiative divertor scenarios.

To address these needs, experiments with nitrogen injection in type-I ELMy H-mode plasmas were conducted in JET, operating with the plasma facing component (PFC) material configuration foreseen in ITER (JET-ILW): full tungsten divertor with bulk beryllium main chamber limiters [3, 4, 5]. Scans in deuterium fuelling (0.8 – 3e22electrons/s) and nitrogen injection (0 – 4e22e/s) were carried out in semi-horizontal low-field side (LFS) divertor, high triangularity, configuration. These experiments were executed at a plasma current of 2.5MA and a toroidal magnetic field of 2.65T, and with about 16 MW of neutral beam heating. Deuterium was injected from the high- field side (HFS) divertor target, and nitrogen was seeded from the LFS divertor target into the common-flux region. These plasmas achieved LFS divertor detachment with inter-ELM radiated power fraction of about 55%. The plasmas exhibited low frequency ELMs in the range of 10 – 50Hz [3, 4]. In this study, the radiative divertor characteristics in these plasmas are further analysed and interpreted with simulations conducted with the multi fluid code EDGE2D-EIRENE [6, 7, 8].

2. EDGE2D-EIRENE SETUP FOR RADIATIVE DIVERTOR INVESTIGATIONS IN JET-ILW H-MODES

EDGE2D-EIRENE was executed for steady state, inter-ELM state of the nitrogen seeded JET-ILW H-mode plasmas. The primary purpose of running these simulations is to identify the dominant radiators and to determine whether the experimentally observed divertor radiation distribution and reduction of the LFS divertor power deposition and particle flux with increasing nitrogen seeding can be reproduced. The input power was set to 8 MW corresponding to the estimated power crossing the separatrix between ELMs: 7 – 9 MW [3, 4]. The cross-field transport parameters for particle diffusion and thermal conduction were adjusted to mimic the pedestal profiles in the unseeded reference plasmas (figure 1). In the divertor plasma below the X-point, radially constant heat conductivities ($1m^2/s$) and particle diffusivities ($0.64m^2/s$) were used to limit the extent of the assumed edge transport barrier to the main scrape-off layer (SOL) and in core plasma regions. Since the scaling of the cross-field transport coefficient with the plasma parameters is not modelled self-consistently in EDGE2D-EIRENE, the cross-field transport parameters are kept fixed through the nitrogen injection scans. Therefore, the model is not capable of capturing the experimentally observed enhancement of pedestal pressure following nitrogen injection. Due to numerical stability issues, the simulations were conducted without cross-field drift terms thus far. Deuterium molecules were injected into the computational domain from the HFS divertor target with feed forward fuelling level, 1.5e22 e/s, adjusted to produce LFS SOL regime in line with Langmuir Probe measurements (table 1). The total simulated radiated power in the computational domain (0.95MW) was a factor of 2 lower than the value measured experimentally (1.5 – 2MW). Similar discrepancies have been documented for JET-ILW L-mode simulations conducted with EDGE2D- EIRENE [12]. Comparison to line integrated bolometer channels indicate that most of the underestimation occurs within the HFS divertor, while in the LFS divertor, the overall radiated power levels are underestimated by of about 20% only. Consistent with the underestimated radiation, the total LFS divertor power deposition was overestimated by 10 – 30% compared to values measured by Langmuir Probes in the unseeded plasmas. Attributed to the overestimated LFS target power deposition, the total integrated divertor particle fluxes in the unseeded plasmas were overestimated by 20 – 30%.

Nitrogen was injected into the computational domain from the LFS divertor target, with injection rate adjusted to produce the radiated power levels observed experimentally. Therefore, any radiation missing in the unseeded simulations in this study is compensated by extra nitrogen radiation in the seeded simulations. As a result, the simulations tend to overestimate divertor NII emissivities at matching radiation levels, which indicates that extra nitrogen radiation indeed compensates the underestimated deuterium and beryllium radiation levels. However, at high radiative fractions, nitrogen is anticipated to be the dominant radiator in the plasma, and the fractional excess of nitrogen content is, therefore, expected to reduce with increasing radiation levels. By the time of conducting this work, EDGE2D-EIRENE was not suitable of injecting nitrogen molecules. However, ERO simulations, including N_2 dissociation physics, indicate that the impact of neglecting nitrogen molecular

dissociation on the singly ionized nitrogen density distribution in the divertor plasma is less than 5%. Therefore, the lack of nitrogen molecular dissociation is not anticipated to be the dominating source of uncertainty in the simulations. Nitrogen surface chemistry is not modelled by EDGE2D-EIRENE. Instead, by the time of conducting this work, only full or zero recycling options were available for impurities. This corresponds to assumption of either 0% or 100% sticking of nitrogen atoms and ions to the wall material. Since nitrogen is chemically active, forming compounds with tungsten, the surface sticking coefficient is expected to be in between these two extreme cases and vary spatially [13]. As a result, the lack of nitrogen surface chemistry is foreseen as a source of uncertainty in the simulations. Therefore, both full and no recycling assumptions are investigated in this study to provide understanding of the sensitivity of the plasma solution on this boundary condition.

Full beryllium main chamber PFCs were assumed, while the divertor target and baffles were assumed to consist of pristine tungsten surfaces. As impurity species, beryllium and nitrogen atoms and ions were included in the simulations, while tungsten was neglected, since EDGE2D-EIRENE is only capable of handling two impurity species. The residual carbon impurity population was also neglected in the simulations, justified by low carbon contamination levels measured experimentally [14]. The EIRENE model used in these studies includes both elastic and inelastic collisions between deuterons and deuterium molecules, collisional-radiative rates describing reactions between electrons and deuterium molecules, and reactions involving deuterium radicals (D_2^+) as described in [15].

3. LOW FIELD SIDE DIVERTOR HEAT LOAD MITIGATION AND INCREASE OF SCRAPE-OFF LAYER RADIATION WITH N_2-INJECTION

The experimentally observed reduction in the LFS target power deposition with increasing divertor radiation is also recovered by the simulations (figure 2a). Both simulations and experimental data show a factor of 10 reduction in the LFS target power deposition when the normalized divertor radiation, $P_{\text{rad divervtor}}/P_{\text{SOL}}$, increases from the unseeded levels of 15% up to the 50% levels required for detachment. Both full and zero nitrogen recycling simulations show a transition to detachment at the LFS target, indicated by detachment of the deuterium ionization front, when less than 10% of the power crossing the separatrix is deposited on the LFS divertor target, consistent with experimental observations (figure 2 a, d).

At the radiation levels required for detachment, nitrogen radiates of about 85% of the total radiated power with deuterium providing 10% and beryllium of about 5% of radiation (figure 2b). This is consistent with spectroscopic studies conducted in JET-C, where nitrogen was also identified as the dominant radiator in nitrogen seeded H-mode plasmas at the radiation levels required for detachment [16]. Also, previous EDGE2D-EIRENE investigations of nitrogen seeded H-modes in JET-C indicated that nitrogen dominated radiation at high radiative fractions [17, 18]. The simulations indicate that while nitrogen radiation is increased with increasing nitrogen injection, the deuterium and beryllium radiation are reduced, further enhancing the dominance of nitrogen as the main radiator in these plasmas (figure 2b). The overall beryllium radiation is reduced from about 0.15

MW in the unseeded cases down to about 0.1MW at highest simulated nitrogen injection levels, and is, therefore, on a negligible level throughout the simulated scans. This is due to low radiative potential of beryllium. The reduction is mainly driven by reduction in the simulated beryllium content in the plasma. The deuterium radiation is reduced with increasing nitrogen injection from the 0.8MW level in the unseeded cases down to 0.2 – 0.3MW at the highest simulated nitrogen injection levels, mainly due to reduced overall deuterium recycling rate.

Due to low radiative potential of nitrogen at electron temperatures above 100, more than 80% of the nitrogen radiation occurs in the SOL in the simulations. Therefore, the simulations indicate that nitrogen is a suitable divertor radiator for typical JET H-mode conditions (figure 2c). Simulations with neon injection with otherwise similar input parameters show linear increase of radiation inside the separatrix with SOL radiation. This is due to significantly stronger radiative potential of neon at electron temperatures between the separatrix, ~ 100eV, and the pedestal, ~ 600eV, in the simulations. The simulated nitrogen radiation inside the separatrix reaches 10% of the power crossing the separatrix only at detached LFS divertor conditions. In these conditions, the concentrations of low charge state nitrogen ions inside separatrix at the X-point increases due to reduced nitrogen ionization to higher charge states in the divertor leg (figure 2 c, d). This leads to increase of the non-coronal nitrogen radiation inside the X-point where the electron temperatures in the steady state simulations in this study stay above 75eV.

4. DISTRIBUTION OF DIVERTOR RADIATION WITH NITROGEN INJECTION

While the unseeded plasmas in this series of discharges radiated dominantly at the HFS divertor, the strongest increase in radiation with nitrogen injection occurred at the LFS divertor, where the nitrogen injection was conducted (figure 3). This is observed both in the 2D bolometric reconstruction of the divertor radiation and in the measured values of the individual bolometer chords. Consistently, the NII (500nm) emissivity distribution in the divertor is also peaked at the LFS divertor (figure 4).

Low-N_2 injection (~ 1.5e22 e/s) leads to a factor of 2 – 3 increase in the LFS divertor radiated power, with the peak of the radiation distribution located in front of the target plate. Simultaneously, transition to high recycling conditions is observed at the LFS divertor as the peak electron temperature drops from about 30eV down to 10eV and the peak ion saturation current increases from 0.6MA/m^2 up to 2 – 3MA/m^2. With medium-N_2 injection (~ 2.5e22 e/s), a further factor of 2 radiated power increase is observed in the LFS divertor leg with a simultaneous shift of the peak emission zone from the LFS strike point to the LFS X-point, while the plasma conditions in the LFS divertor remained still high recycling. Finally, with the highest N_2 injection (~ 3.5e22 e/s), detachment of the LFS divertor radiation front and shift to the LFS X-point is indicated by both the bolometric reconstruction and individual bolometer chords. Simultaneously, the peak LFS target saturation current is reduced below 0.5MA/m^2 indicating transition to detached divertor conditions. The peak electron temperatures, measured with the divertor Langmuir Probes, saturate around 5 – 10eV. However, as will be shown in this paper, visible nitrogen spectroscopy of NII (500nm) line emission

coupled to EDGE2D-EIRENE simulations indicate that the electron temperatures in front of the LFS target in these nitrogen induced detached conditions are well below 5eV, presumably in the range of ~ 0.5eV.

The simulations show also increase in the LFS divertor radiation with the peak of the radiation distribution located in front of the strike point with nitrogen injection in high recycling conditions (figure 5 a, c). The simulations indicate that this is due to strong radiative potential of nitrogen in the 10 – 30eV electron temperatures relevant for high recycling conditions in the LFS divertor leg. The total power deposition at the LFS divertor can be reduced by a factor 3 – 5 in high recycling conditions compared to the unseeded simulations.

With the onset of detached LFS divertor conditions, the simulations also show a shift of the nitrogen radiation front from the LFS divertor leg to the LFS X-point (figure 5b, d). This is due to shift of the 10 – 30eV electron temperature front from the divertor leg to next to the X-point. Close to the LFS X-point, this electron temperature front is stabilized due to shallow magnetic pitch angle and cross-field heat source from the confined plasma. As a result of the shallow magnetic pitch angle at the X-point, the poloidal range, within which the parallel electron temperature profile spans the 10 – 30eV range, is contracted. Significant reduction of the parallel heat conductivity, expected with increasing impurity concentration [2], and associated steepening of the parallel temperature gradients does not occur in the simulations. This is due to increasing electron density with reducing temperature in the radiation front following increasing nitrogen density and radiation. As a result, the effective charge state in the radiation zone in the simulations is not increased significantly during the nitrogen injection scan. The simulations indicate that the peak power flux reduction in the nitrogen induced detached conditions is obtained almost solely via nitrogen radiation. The deuterium radiation densities along the separatrix predicted by the code are 1 – 2 orders of magnitude lower than those of nitrogen. In these conditions, a factor of 20 reduction of the total LFS target power deposition compared to the unseeded plasmas is obtained in the simulations.

In high recycling LFS divertor conditions, across the LFS divertor, both the full and zero nitrogen recycling simulations reproduce the experimentally measured radiated power signals of the vertical bolometer system mainly within the error bars and with the peak value overestimated by 20 – 30% (figure 5a). At the HFS divertor, the zero recycling model underestimates the emitted radiation by a factor of 2, while the full recycling model predicts radiative values of a factor 2 higher than measured. Consistently, the full recycling model overestimates the HFS divertor NII (500nm) emissivities by a factor of 2 – 5, while the zero recycling model predicts zero nitrogen densities and NII emissivities at the HFS. The latter provides a strong argument for the presence of nitrogen recycling source in the HFS divertor, while the full recycling model presumably overestimates this source.

In detached conditions, both the full and zero recycling simulations show divertor radiation values within the error bars of the vertical bolometer (figure 5 b). Due transparency of the LFS divertor for nitrogen atoms in detached conditions, even with zero recycling assumption, nitrogen transport from the LFS divertor to HFS divertor is sufficient to produce HFS divertor radiated power levels

seen experimentally. However, comparison to NII (500 nm) emissivities in the HFS divertor show that the amount of low charge nitrogen ions close to the HFS baffle is still underestimated without recycling. Assuming full recycling, the HFS NII emissivities in the HFS divertor leg are a factor of 3 – 10 higher than measured.

Since the NII emission peaks at around electron temperatures of 5 – 15eV, it is a good indicator for the poloidal location of the deuterium ionization front, $T_e > 5$eV, as is shown by the simulations (figure 5 e – h). Visible divertor spectroscopy for NII line emission at 500 nm indicates that, at low-N_2 injection levels, the NII emission is localized close to the seeding location at the LFS target (figure 2). This is consistent with attached high recycling divertor conditions with target electron temperatures in the range of 5 – 15eV, as is also indicated by the simulations (figure 5e). Increasing seeding to the medium-N_2 levels leads to a shift of the NII emission zone half-way up the LFS divertor leg towards the X-point, indicating a shift of the $T_e \sim 5 – 15$eV front upwards in the divertor leg, while the divertor conditions are still high recycling. At the high-N_2 level, the emission zone is observed to be detached from the targets and shifted to the LFS X-point, indicating detachment of the $T_e \sim 5 – 15$eV front consistent with detached divertor conditions and detachment of the total radiated power front, as is also seen in the simulations.

5. REDUCTION OF THE LOW-FIELD SIDE PLATE PARTICLE FLUXES AT THE ONSET OF NITROGEN INDUCED DETACHMENT

The simulations capture the experimentally measured LFS plate ion saturation currents in the high recycling and detached conditions mainly within the experimental error bars (figure 6). However, with the full nitrogen recycling assumption, the peak ion saturation current in the high recycling conditions was underestimated by a factor of 2. This is due to sensitivity of the deuterium ionization distribution in front of the target to the nitrogen density and radiation distribution, which depends strongly on the assumption on nitrogen recycling.

Simulations without 3-body and radiative volume recombination processes indicate that a factor of 2 – 3 particle flux and peak pressure reduction can be achieved even without volumetric losses for particles (figure 6). This is due to a factor of 2 – 3 reduction of the overall recycling levels in the LFS divertor leg with transition to detached conditions. The simulations indicate that the reduction of recycling levels occurs due to combination of low power levels entering the deuterium ionization front and momentum losses in the divertor leg. The first one reduced the overall ionization rate, while the latter limits the plasma flow into the recombination zone close to and at the target, reducing the overall deuterium recombination rate, such that particle balance is maintained. The effective charge states in front of the targets in the simulations stay below 1.05. Therefore, the simulated plasma flux to the target is strongly dominated by fuel species, and the true integral particle flux to the target is indeed reduced.

This lowered recycling state is possible due to the nitrogen radiation front located at the LFS X- point in the common SOL, reducing the parallel power flow into the divertor leg by more than a

factor of 10. Therefore, strong electron cooling via deuterium ionization and radiation is not needed to cool the divertor plasma such that ion-neutral friction can become effective to support parallel plasma pressure gradients in the divertor leg [19 – 22]. As a result, the deuterium ionization rate can be reduced without violating the need for increasing power dissipation, required for detached conditions. Both the full and zero nitrogen recycling simulations indicate that a parallel pressure difference of 500 – 1000Pa between the ionization front, located below the X-point, and the target is generated. The outer mid-plane pressures in these conditions are predicted to be reduced by about 10% compared to the high recycling conditions. As a result of the pressure loss in the divertor leg, the total particle flow into the recycling zone in the divertor leg and the total volumetric and surface recycling rate is reduced, following the physics mechanisms described in [19]. This reduction is sufficient to produce most of the experimentally observed pressure and particle flux reduction at the LFS target. Finally, in front of the targets, the recombination rates are predicted to become comparable to the plasma particle flux when the electron temperatures drop down to below 0.5 eV, providing access to deep detachment with integrated surface particle fluxes of a factor of 5 lower than in the attached high recycling simulations (figure 6). However, the bulk reduction in the plate particle fluxes is obtained already due to reduced LFS divertor recycling.

The reduced overall recycling is presumably one of the key features separating impurity radiation induced detachment from deuterium fuelling induced detachment, since in the latter the main power dissipation mechanism, deuterium ionization and radiation, is coupled to the recycling process itself. Therefore, deuterium fuelling induced detachment cannot necessarily easily satisfy the simultaneous requirements for increasing power dissipation with reducing surface recycling without invoking strong volume recombination source of neutral deuterium. In the impurity induced detachment, on the other hand, the overall deuterium recycling rate can be reduced with increasing volumetric power losses due to decoupling of the recycling rate and power dissipation. However, this requires spatial separation of the deuterium ionization front from the radiative power exhaust front, to reduce the parallel heat-flux before it reaches the neutral deuterium population.

CONCLUSIONS

The experimentally observed factor of 10 reduction in the LFS target power deposition is also predicted in nitrogen seeded JET-ILW H-mode plasmas when the normalized divertor radiation, P_{rad} div / PSOL, increases from the unseeded levels of 15% up to the 50% levels. Consistent with previous experimental measurements in JET-C, nitrogen is predicted to be the dominant radiator at radiation levels required for detachment. At the radiation levels required for detachment, nitrogen provides 85% of the total radiation, with deuterium providing 10% and beryllium the remaining 5% of radiation. The simulations show that due to low radiative potential of nitrogen in electron temperatures above 100 eV, more than 80% of the nitrogen radiation occurs outside the separatrix in the simulations, making nitrogen a suitable divertor radiator for typical JET conditions. Simulations with neon seeding with similar input parameters show linear increase of radiation inside the

separatrix with SOL radiation due to significantly stronger radiative potential of neon in electron temperatures above 100eV.

The simulations reproduce the experimentally observed increase in the LFS divertor radiation with nitrogen seeding, and the radiation peaking at the LFS X-point with the transition to LFS divertor detachment. The simulations also reproduce the experimentally observed shift of NII (500nm) emission peak from the LFS strike point with the onset of detachment and indicate that the location of the NII peak is a good proxy for the poloidal location of the deuterium ionization front. Therefore, the NII emission distribution can be used to extract 2-D information about the divertor electron temperatures.

The experimentally observed reduction in the LFS target particle fluxes with nitrogen induced detachment is also seen in the simulations. The simulations indicate that this is due to both reduced overall deuterium recycling rate, by a factor of 2 – 3, in the LFS divertor, and due to volume recombination in front of the target. The reduction of the recycling rate can occur due to low power levels entering the deuterium recycling front, and is, therefore, strongly linked to the extrinsic impurity radiation. As a result, this mechanism is not expected to apply in fuelling to detachment, since without strong impurity radiation, the main power dissipation mechanism, deuterium ionization and radiation, is coupled to the recycling process itself.

ACKNOWLEDGEMENTS

This work, supported by the European Communities under the contract of association between EURATOM/TEKES was carried out within the framework of the European Fusion Development Agreement. The views and opinions expressed herein do not necessarily reflect those of the European Commision. The work was also partly funded by the Academy of Finland under the Grant number 13253222.

REFERENCES

[1]. A. Loarte, et al. Nuclear Fusion **47**, (2007), S203 – S263
[2]. A. Kallenbach, et al. Plasma Physics and Controlled Fusion **55**, (2013), 124041
[3]. C. Giroud, et al. Nuclear Fusion **53**, (2013), 113025
[4]. G. Maddison, et al. Nuclear Fusion, in Press
[5]. G.F. Matthews, et al. Journal of Nuclear Materials **438**, (2013), S2 – S10
[6]. R. Simonini, et al. Contributions to Plasma Physics **34**, (1994), 368 – 373
[7]. D. Reiter, Journal of Nuclear Materials **196 – 198**, (1992), 80 – 89
[8]. S. Wiesen, EDGE2D/EIRENE code interface report, JET ITC-Report, http://www.eirene.de/e2deir_report_30jun06.pdf, 2006
[9]. M. N. A. Beurskens, et al. Nuclear Fusion **48**, (2008), 095004
[10]. M. Brix, et al. Review of Scientific Instruments **83**, (2012), 10D533
[11]. R. D. Monk, et al. Journal of Nuclear Materials **241 – 243**, (1997), 396

[12]. M. Groth, et al. Nuclear Fusion **53**, (2013), 093016
[13]. M. Oberkofler, et al. Journal of Nuclear Materials **438**, (2013), S258 – S261
[14]. S. Brezinsek, et al. Journal of Nuclear Materials **438**, (2013), S303-S308
[15]. V. Kotov, et al. Plasma Physics and Controlled Fusion **50**, (2008), 105012
[16]. C. Maggi, et al. Journal of Nuclear Materials **241 – 243**, (1997), 414.
[17]. D. Moulton, et al. Journal of Nuclear Materials **S509–S512**, (2011), 415.
[18]. D. Moulton, PhD Thesis, Numerical Modelling Of H-mode Plasmas on JET, Imperial College London, Department of Plasma Physics, 6.12.2011
[19]. P. C. Stangeby, et al. Nuclear Fusion **33**, (1993), 11
[20]. M. Wischmeier, et al. Journal of Nuclear Materials **390 – 391**, (2009), 250 – 254
[21]. D. Post, et al. Physics of Plasmas **2**, (1995), 2328
[22]. A. Kallenbach, et al. Journal of Nuclear Materials **415**, (2011), S19 – S26
[23]. A. Huber, et al. Review of Scientific Instruments **83**, (2012), 10D511
[24]. P. D. Morgan, et al. Review of Scientific Instruments **56**, (1985), 862

	T_e^{OT} [eV]	$J_{sat,peak,\ OT}$ [MA/m^2]	$I_{LFS,\ DIV}$ [1e23 e/s]	$q_{peak,\ OT}$ [MW/m^2]	P_{OT} [MW]
Experiment	30 +/– 15	6 + /– 1	2.3 +/– 0.2	2.7 +/– 1	2.5 – 3
EDGE2D-EIRENE	35	7.5	2.9	2.5	3.44

Table 1. Comparison of the outer target electron temperature, T_e, peak saturation current, J_{sat}, integrated particle flux, $I_{LFS,\ DIV}$, peak heat flux, q_{peak}, and total heat deposition, P_{OT}, in the unseeded plasmas as measured by target Langmuir Probes [11] and predicted by EDGE2D-EIRENE.

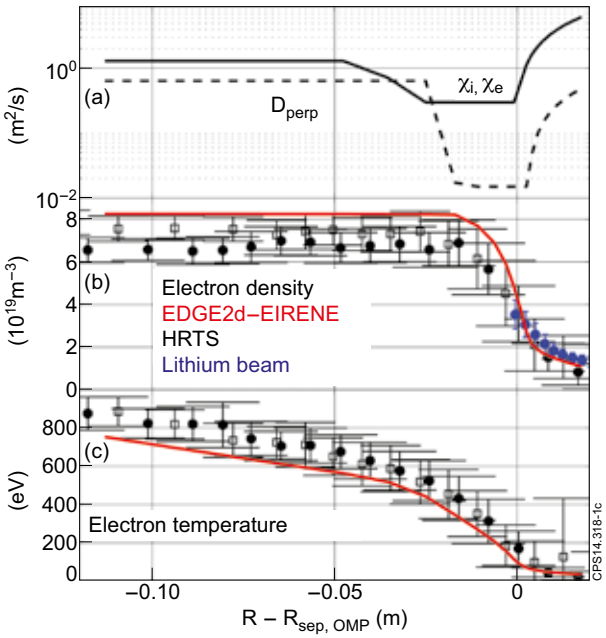

Figure 1. a) The cross-field transport coefficient for electron and ion heat conduction (χ_e, χ_i), and for particle diffusion (D_{perp}). b) The outer mid-plane electron density profile as measured by the high resolution Thomson scattering (HRTS) [9] (black), Lithium beam [10] (blue), and simulated by EDGE2D-EIRENE (red). The solid squares are measurement points from JET Pulse Number: 85406, and the hollow squares from JET Pulse Number: 82806. c) The electron temperature profiles at the outer mid-plane.

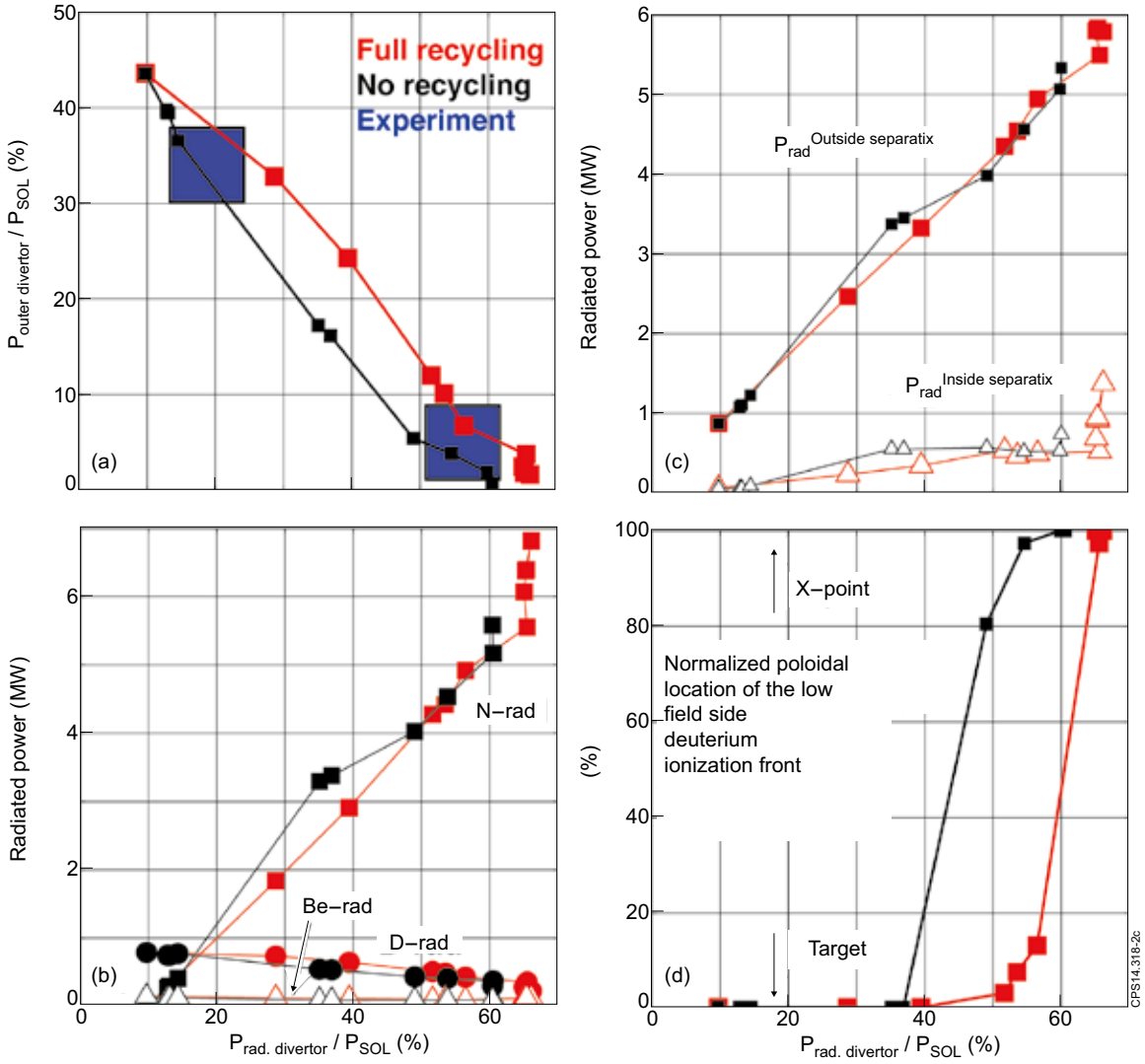

Figure 2. a) Reduction of the normalized LFS divertor power deposition with increasing divertor raditation below Z = -1.2 m. P_{SOL} stands for power crossing the separatrix. The blue squares represent experimental data points, with the estimated error illustrated by the size of the symbol.
The red symbols stand for the full nitrogen recycling series, and the black symbols for the zero nitrogen recycling series. b) Simulated total radiated power due to nitrogen (squares), deuterium (circles), and beryllium (triangles). c) Simulated radiated power inside and outside the separatrix. d) Normalized poloidal location of the simulated deuterium ionization front in the LFS divertor leg: 0% stands for the target, and 100% for the X-point.

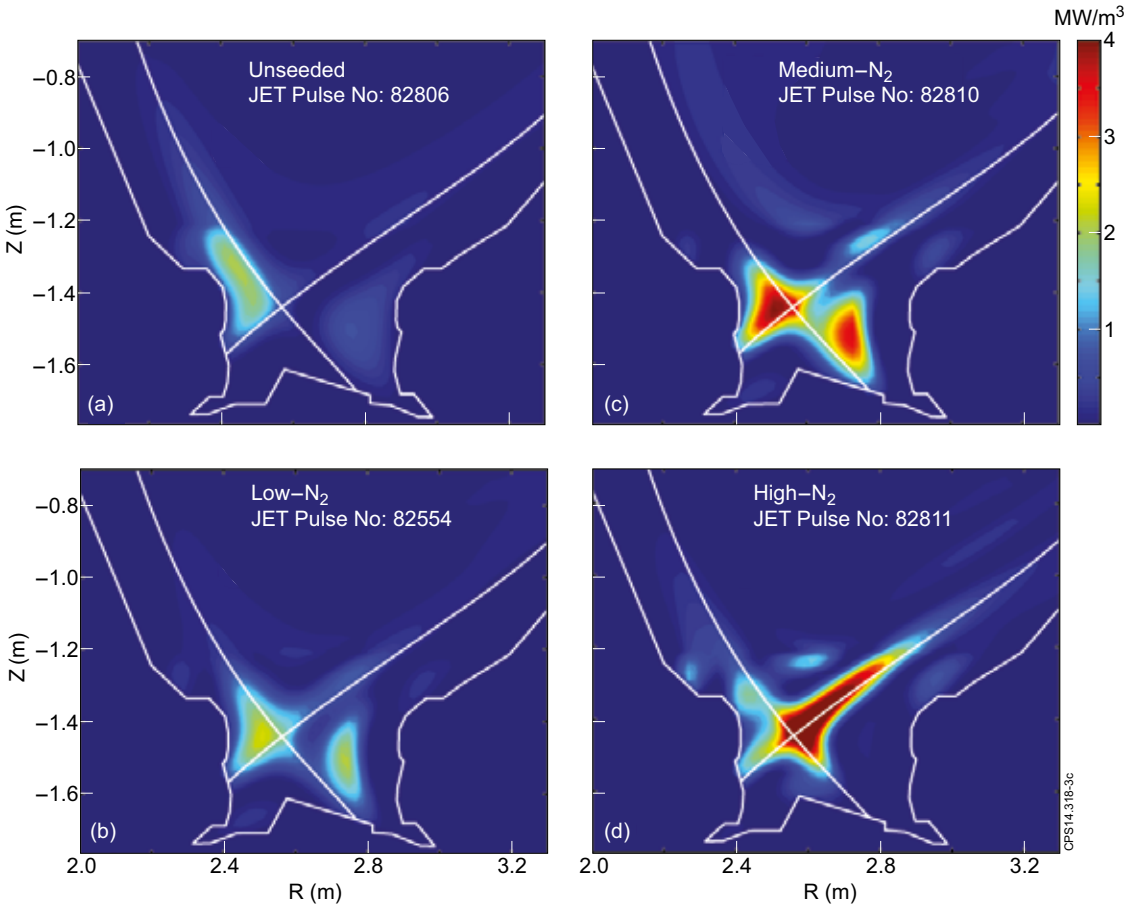

Figure 3. 2-D bolometric reconstructions of radiated power for the investigated JET plasmas: unseeded (Pulse No: 82806), low seeding (~ 1.5e22 e/s) (Pulse No: 82554), medium seeding (~ 2.5e22 e/s) (Pulse No: 82810), and high seeding (~ 3.5e22 e/s) (Pulse No: 82811).

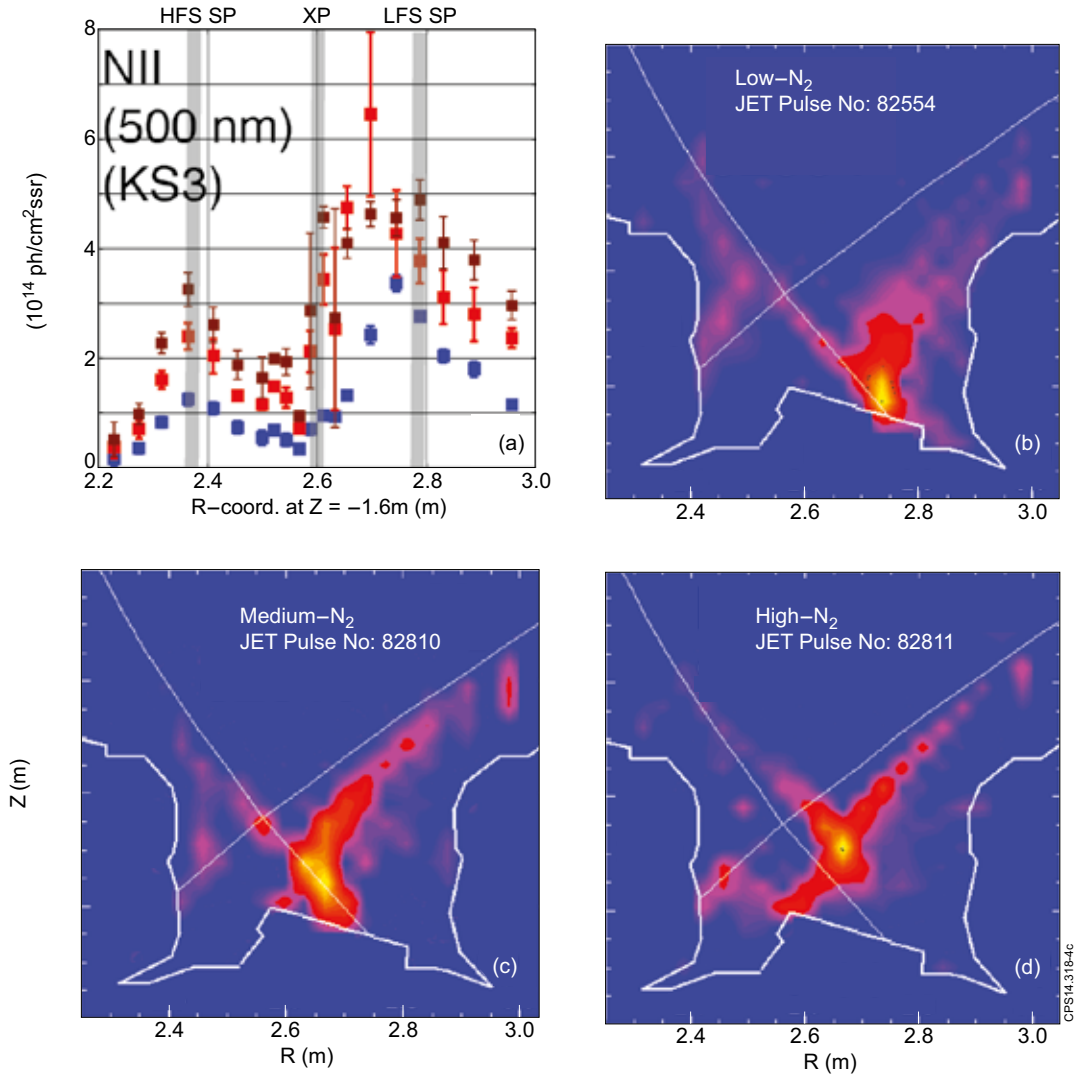

Figure 4. Nitrogen NII (500 nm) spectroscopic signals in the divertor. a) Line-integrated NII emissivities in the divertor as measured by the vertical divertor spectrometer (JET diagnostics system KS3) [24]. The radial locations of the HFS strike point (HFS SP), X-point (XP), and LFS strike point (LFS SP) are illustrated with grey shading. b – d) 2D reconstructed NII emission in the divertor plasma, based on the divertor endoscope measurements (JET diagnostic system KL11) [23].

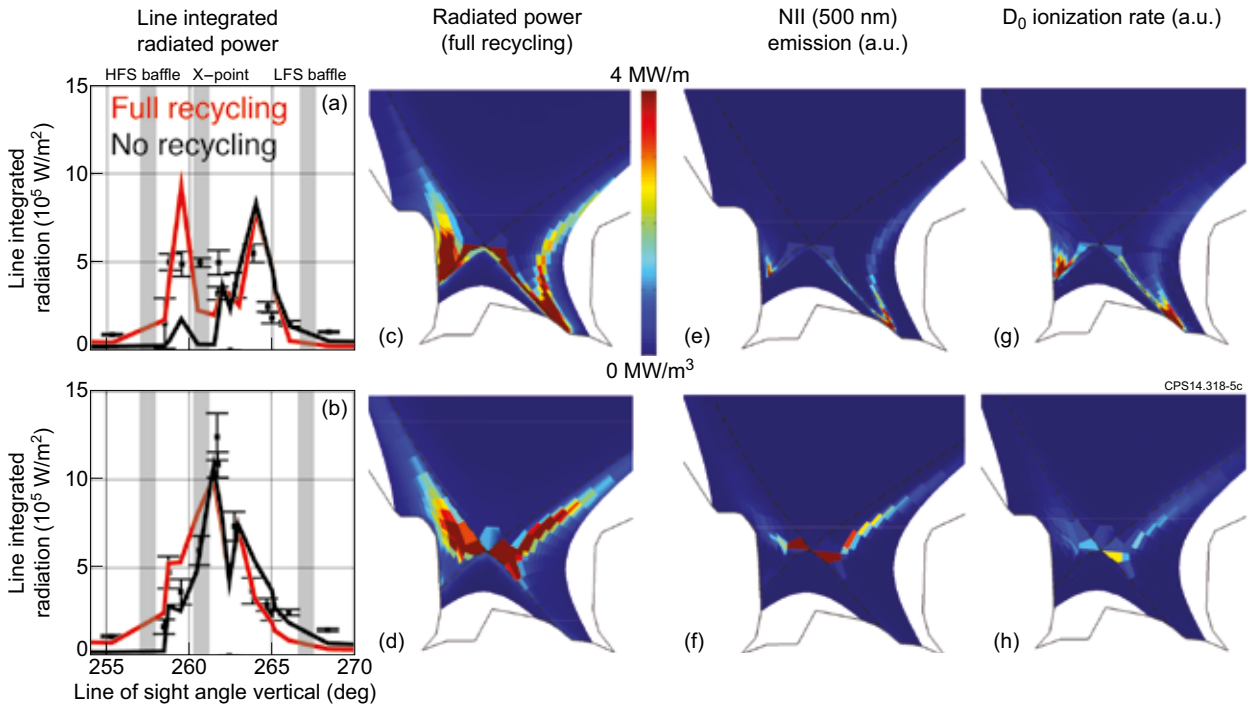

Figure 5. a – b) Comparison of the simulated divertor channels of the vertical bolometry for attached high recycling (a) and detached (b) conditions. Low-N_2 (Pulse No: 82554) and high-N_2 (Pulse No: 82811) are used for the experimental data. The red lines stand for EDGE2D-EIRENE simulations with full recycling assumption for nitrogen and the black lines for EDGE2D-EIRENE simulations with zero recycling assumption for nitrogen. Simulated 2-D radiated power distribution (b, c), 2-D NII emission distribution (e, f), and 2-D deuterium ionization distribution (g, h) for attached and detached EDGE2D-EIRENE simulations with full recycling assumption. In the radiated power figures, the color bar spans from 0 (blue) to 4 MW/m^3 (red). Arbitrary units are used in the NII emission and D_0 ionization distribution figures.

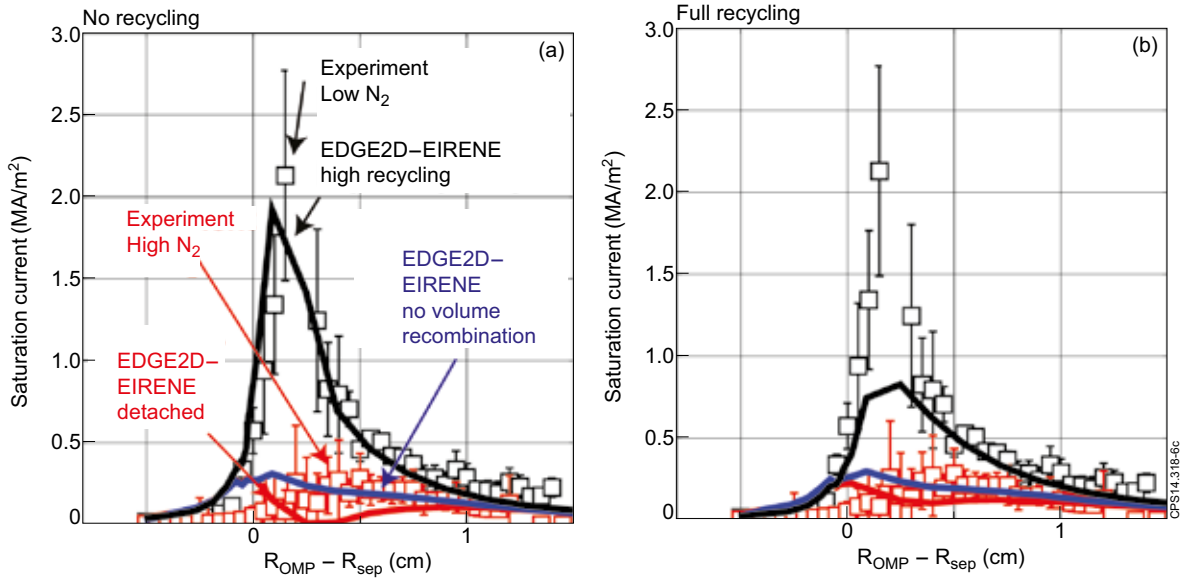

Figure 6. Simulated outer divertor ion saturation currents before and after nitrogen induced detachment with zero recycling assumption for nitrogen (a) and with full recycling assumption for nitrogen (b). Black symbols represents plasmas in high recycling conditions (Pulse No: 82554) and the red symbols stands for plasmas in detached conditions (Pulse No: 82811). Blue curves represent EDGE2D- EIRENE simulations without 3-body, and radiative volume recombination processes.